Articles

Synthesis, Thermal Behavior, and Structure of Hexaaquanickel(II) Chloro(hydrogenethylenediaminetetraacetato)ferrate(III): A Molecular Precursor for Stoichiometric Nickel Ferrite

Allen W. Apblett,* Luis A. Cubano, Galina D. Georgieva, and Joel T. Mague

Department of Chemistry, Tulane University, New Orleans, Louisiana 70118

Received August 2, 1995. Revised Manuscript Received November 20, 1995[⊗]

Hexaaquanickel(II) chloro(hydrogenethylenediaminetetraacetato)ferrate(III), $[Ni(H_2O)_6][FeCl(EDTA)H]_2 \cdot 4H_2O$, was prepared by the reaction of nickel(II) chloride with (hydrogenethylenediammine)iron(III) in water at room temperature. The compound readily loses water at room temperature depending on drying conditions and the relative humidity. The molecular structure of the dihydrate was determined by single-crystal X-ray crystallography. The compound decomposes in stages involving, successively, loss of water, pyrolysis of the EDTA ligand, and loss of HCl to yield, finally, stoichiometric nickel ferrite. Crystal data: $C_{20}H_{42}N_4O_{24}Cl_2Fe_2Ni$, $M = 963.88$, monoclinic, space group $P2_1/c$, $a = 20.548(3)$ Å, $b = 7.401(1)$ Å, $c = 12.827(1)$ Å, $\beta = 101.78(1)°$, $V = 1909.6(7)$ Å^3, $Z = 2$, $D_{calc} = 1.68$ g cm^{-3}, $R = 0.028$, and $R_w = 0.040$.

Introduction

Spinel ferrites, MFe_2O_4 (M = Mg, Mn, Fe, Co, Ni, Zn, Cu, Cd, etc.), combine a wide range of useful magnetic properties with relatively low electrical conductivity. Thus, unlike magnetic metals and alloys, they display low eddy current loss in alternating current applications and they are particularly useful in the radio frequency range. Therefore, the spinel ferrites have numerous applications in recording heads, core materials for various transformers, inductors, and TV deflection units, and recording tape.[1]

Most ferrites are prepared by reacting intimate mixtures of the constituent metal oxides or carbonates. The shortcomings of such an approach include the formation of relatively coarse particles leading to large and inhomogeneous porosity in sintered bodies, incomplete reaction of the oxide powders, and limitations on the ability to control composition.[2] One way to closely approach the ideal ratio of one divalent metal ion per two ferric ions required by ferrites is to use a precursor that crystallizes with the correct stoichiometry. The best example of a precursor which fixes the stoichiometric ratios of two metals in a bimetallic ceramic oxide is barium titanyl oxalate (BTO), $BaTi(O)(C_2O_4)_2 \cdot 5H_2O$. As early as 1956, Clabaugh et al. reported the great utility of this compound for the preparation of stoichiometric barium titanate.[3] Since that time, this application of BTO has been the subject of over 40 patents and publications. Surprisingly, however, it was not until 1992 when the crystal structure of BTO was reported-confirming the presence of a crystalline compound with a 1:1 barium:titanium ratio.[4]

In the case of ferrites, it has been demonstrated that Fe^{2+} and M^{2+} may be coprecipitated from solution by treatment with oxalic acid.[5] These solid solutions of divalent metal oxalates could subsequently be converted to ferrites by thermal decomposition of the anion and oxidation of Fe^{2+} to Fe^{3+} (requiring temperatures of 800−1000 °C). However, the differences in solubility of the Fe^{2+} and M^{2+} oxalates and their tendency to form supersaturated solutions leads to a fair amount of deviation in the Fe:M ratio unless the reaction conditions are carefully controlled.[5]

An excellent example of crystalline precursors for stoichiometric ferrites is the mixed acetates, $M_3Fe_6(CO_2CH_3)_{17}O_3(OH) \cdot 12$pyridine (M = Ni, Co, Mn) reported by Wickham et al.[6] Heating these precursors in the range 800−1100 °C yielded the respective ferrites in which the iron-to-divalent metal atomic ratio deviates less than 0.01 from the ideal value of 2. While the mixed acetates were easily recrystallized, this process had the drawbacks of requiring pyridine. As well, the pyridines of crystallization had to be carefully removed in order to avoid melting of the crystals and consequent segregation

[⊗] Abstract published in *Advance ACS Abstracts,* February 1, 1996.

(1) Kools, F. X. N. M.; Stoppels, D. Ferrites. In *Kirk-Othmer Encyclopedia of Chemical Technology,* 4th ed.; Kroschwitz, J. I., Howe-Grant, M., Eds.; John Wiley and Sons: New York, 1991.
(2) Johnson, D. W.; Ghate, B. B. In *Advances in Ceramics*; Wang, F. Y., Ed.; American Ceramic Society; Columbus, OH, 1985; Vol. 15, pp 27−38.
(3) Clabaugh, W. S.; Swiggard, E. M.; Gilchrist, R. *J. Res. Natl. Bur. Stand.* **1956**, *56*, 289.
(4) Rhine, W. E.; Hallock, R. B.; Davis, W. M.; Wong-Ng, W. *Chem. Mater.* **1992**, *4*, 1208.
(5) Wickham, D. G. *Inorg. Synth.* **1967**, *9*, 152.
(6) Wickham, D. G.; Whipple, E. R.; Larson, E. G. *J. Inorg. Nucl. Chem.* **1960**, *14*, 217.

0897-4756/96/2808-0650$12.00/0

of the metal ions. Therefore, we have been developing alternative precursors to stoichiometric ferrites that may be synthesized in and recrystallized from water. One iron compound that would upon first examination appear to be ideally suited for preparation of a ferrite precursor is sodium iron ethylenediamine tetraacetate (NaFeEDTA). This compound would be expected to react with a divalent metal chloride to produce sodium chloride and $M[Fe(EDTA)]_2$. In practice, however, the replacement of sodium ions with a divalent metal ion such as Ni^{2+} is incomplete, and compounds containing sodium and a correspondingly decreased amount of divalent metal are obtained. A similar problem with the preparation of $BaTiO(oxalate)_2$ from $K_2TiO(oxalate)_2$ and $BaCl_2$ has been previously observed. We have demonstrated that one solution to this problem for BTO is to replace the potassium ions with protons using a cationic ion exchanger.[7] The "$H_2TiO(oxalate)_2$" thus produced then reacted cleanly with $BaCl_2$ to yield stoichiometric BTO. In a similar approach to a nickel ferrite precursor, using NaFeEDTA and $NiCl_2$, we have prepared the title compound, hexaaquanickel(II) chloro(hydrogenethylenediaminetetraacetato)ferrate(III), $[Ni(H_2O)_6][FeCl(EDTA)H]_2 \cdot XH_2O$ (**1**), which has the desired stoichiometry of the two metals. The results of this investigation, the crystal structure of the precursor, and its conversion to stoichiometric $NiFe_2O_4$ are reported herein. This precursor is simply and inexpensively prepared without resort to nonaqueous solvents, and its conversion to nickel ferrite occurs at similar temperatures as the other known metal carboxylate precursors.

Experimental Section

$NiCl_2 \cdot 6H_2O$ (MCB), $Ni(NO_3)_2 \cdot 6H_2O$ (Mallinckrodt), and NaFeEDTA (Aldrich) were commercial reagents and were used without further purification. Amberlite CG-120 resin (Aldrich) was charged by treatment with 6 M hydrochloric acid followed by washing with distilled water. Infrared spectra were obtained as Nujol mulls or KBr pellets on a Mattson Cygnus 100 FT-IR spectrometer. Metal content was determined by ICP spectroscopy on a Perkin-Elmer Optima instrument or by X-ray fluorescence spectroscopy on a Spectro X-Lab energy-dispersive XRF spectrometer. The latter instrument was also used for determination of chloride content. UV−visible spectra were obtained using aqueous solutions and a Hewlett-Packard 8451A diode array spectrometer. Thermogravimetric studies were performed using 20−30 mg samples in a Seiko TG/DTA 220 instrument under a 100 mL/min flow of dry air. The temperature was ramped from 25 to 625 °C at a rate of 2 °C/min while the off-gases were analyzed on a Fisons Thermolab mass spectrometer. Bulk pyrolyses at various temperatures were performed in ambient air in a temperature-programmable muffle furnace using ca. 2 g samples, a temperature ramp of 5 °C/min and a hold time of 12 h. X-ray powder diffraction patterns were obtained on a Scintag XDS 2000 diffractometer using copper Kα radiation. Microanalysis for C, H, and N content was performed by Oneida Research Services.

Reaction of NaFeEDTA with $Ni(NO_3)_2$. (A) $Ni(NO_3)_2 \cdot 6H_2O$ (3.12 g, 10.7 mmol) was added to a hot solution (90 °C) of NaFeEDTA (8.06 g, 20 mmol) in 20 mL of H_2O. Upon cooling to room temperature, the solution began to deposit yellowish brown crystals. After 12 h the crystals were isolated by filtration and washed with three 20 mL aliquots of ice water followed by three 40 mL aliquots of 95% ethanol. Drying in a vacuum desiccator yielded 4.71 g of yellowish brown crystals. Analysis for metal content by ICP spectroscopy indicated a composition of $Na_{0.91}Ni_{0.04}$(FeEDTA).

(B) $Ni(NO_3)_2 \cdot 6H_2O$ (14.53 g, 50 mmol) was added to a hot solution (90 °C) of NaFeEDTA (4.03 g, 10 mmol) in 20 mL of H_2O. No crystallization was observed upon cooling the solution to 0 °C. Absolute ethanol (300 mL) was added to the reaction mixture, and the resulting solution deposited a large crop of greenish brown crystals upon standing at room temperature. These were isolated by filtration and washed with three 20 mL aliquots of ice water followed by three 40 mL aliquots of 95% ethanol. Drying in a vacuum desiccator yielded 3.82 g of yellowish brown crystals. Analysis for metal content by ICP spectroscopy indicated a composition of $Na_{0.22}Ni_{0.39}$(FeEDTA).

Preparation of $[Ni(H_2O)_6][FeCl(EDTA)H]_2 \cdot 4H_2O$. NaFe(EDTA) (4.03 g, 10 mmol) in 100 mL of H_2O was passed through a 100 mm i.d. column containing 20 g of proton-charged cationic ion exchanger. The yellowish brown eluent was drained directly into a solution of $NiCl_2 \cdot 6H_2O$ (1.19 g, 5 mmol) in 50 mL of water. The ion-exchange column was washed with a further 20 mL of water, and this too was added to the nickel chloride solution. The resulting dark green solution was evaporated to dryness on a rotary evaporator to afford 3.85 g of crude NiFe(EDTA) as a dark-green solid. Recrystallization from 50 mL ethanol:water (1:1) yielded 3.80 g of purified product. Elemental anal. calcd for $C_{20}H_{46}N_4O_{26}NiFe_2Cl_2$: C 24.02%, H 4.63%, N 5.60%, Ni 5.9%, Fe 11.2%, Cl 7.1%. Found: C 23.98%, H 4.60%, N 5.67%, Ni 6.1%, Fe 11.4%, Cl 7.3%. IR (KBr pellet, cm^{-1}) 3498 (s, br), 3294 (s, br), 2993 (w), 2970 (w), 2936 (w), 2886 (w), 2726 (w), 2610 (w), 2546 (w), 2341 (w), 1728 (s), 1675 (vs, sh), 1628 (vs), 1461 (m), 1435 (m), 1369 (vs), 1355 (vs), 1323 (s), 1300 (m), 1273 (w), 1222 (s), 1163 (w), 1097 (s), 1162 (w), 1081 (w), 1046 (w), 998 (m), 963 (m), 933 (s), 893 (w), 866 (m), 804 (m), 761 (m), 726 (m), 652 (w), 581 (w), 547 (w).

X-ray Crystallography. A greenish-orange crystal of $[Ni(H_2O)_6][FeCl(EDTA)H]_2 \cdot 2H_2O$ (**1**), obtained by slow evaporation of an aqueous solution of the complex, was cut to size and mounted on the end of a thin glass fiber with a coating of epoxy cement. General procedures for crystal orientation, unit-cell determination, and refinement and data collection on the Enraf-Nonius CAD-4 diffractometer have been published,[8] while those pertinent to the present structure are given in Table 1. The monoclinic cell obtained by the CAD-4 software was confirmed by the observation of 2/*m* diffraction symmetry and the space group was uniquely determined by the systematic absences in the final data set. The data were corrected for Lorentz and polarization effects, for a linear 2.3% decay in the intensities of the check reflections and for absorption employing ψ scans on four reflections with χ near 90°. The positions of the metal atoms were obtained by direct methods (SIR-88[9]) and the remainder of the structure developed by successive cycles of full-matrix, least-squares refinement followed by calculation of a $\Delta\rho$ map. Following refinement of all non-hydrogen atoms with anisotropic displacement parameters, most hydrogen atoms were visible in a $\Delta\rho$ map. Those attached to oxygen were refined with isotropic displacement parameters while those attached to carbon were placed in calculated positions (C−H = 0.95 Å) with isotropic displacement parameters 20% larger than those of the respective carbon atoms and updated periodically. The neutral atom scattering factors[10] include corrections for the real and imaginary components of the effects of anomalous dispersion.[11] All calculations were performed on a VAXstation 3100 computer with the MoIEN suite of programs.[12] Final, refined param-

(7) Apblett, A. W.; Georgieva, G. D.; Raygoza-Maceda, M. I. *Ceram. Trans.* **1994**, *43*, 73.

(8) Mague, J. T.; Lloyd, C. L. *Organometallics* **1988**, *7*, 983.

(9) Burla, M. C.; Camalli, M.; Cascarano, G.; Giacovsazzo, C.; Polidori, G.; Spagna, R.; Viterno, D. *J. Appl. Cryst.* **1989**, *22*, 389.

(10) Cromer, D. T.; Waber, J. T. *International Tables for X-ray Crystallography*; The Kynoch Press: Birmingham, England, 1974; Vol. VI, Table 2.2B.

(11) Cromer, D. T. *International Tables for X-ray Crystallography*; The Kynoch Press: Birmingham, England, 1974; Vol. IV, Table 3.2.1.

(12) Fair, C. K. *MoIEN, An Interactive Intelligent System for Crystal Structure Analysis*; Enraf-Nonius: Delft, The Netherlands, 1990.

Table 1. Summary of Crystallographic Data

formula	$C_{20}H_{42}N_4O_{24}Cl_2Fe_2Ni$
fw	963.88
cryst size, mm	0.46 × 0.36 × 0.50
cryst system	monoclinic
space group	$P2_1/c$
a, Å	20.548(3)
b, Å	7.4011(7)
c, Å	12.827(1)
β, deg	101.78(1)
V, Å^3	1909.6(7)
Z	2
ρ_{calc}, g cm^{-3}	1.68
μ, cm^{-1}	14.7
range trans factors	0.8571−0.9998
temp, K	293
radtn	Mo Kα (graphite-monochromated, λ = 0.710 73 Å)
scan type	$\omega/2\theta$
2θ range, deg	2.0−52.0
total no. of reflns	4165
no. unique reflns	3737
R_{int}	0.012
no. of obs data	2922 ($I \geq 2\sigma(I)$)
no. of parameters	294
$(\Delta/\sigma)_{max}$ in last cycle	0.12
R^a	0.028
$R_w{}^b$	0.040
GOF^c	1.39
$\Delta\rho$ in final ΔF map, e/Å^3	0.59 to −0.43

^{a} $R = \sum||F_o| - |F_c||/\sum|F_o|$. ^{b} $R_w = [\sum w(||F_o| - |F_c||)^2/\sum w(|F_o|)^2]^{1/2}$ with $w = 1/(\sigma_F)^2$; $\sigma_F = \sigma(F^2)/2F$; $\sigma(F^2) = [(\sigma_I)^2 + (0.04F^2)^2]^{1/2}$. ^{c} GOF $= [\sum w(||F_o| - |F_c||)^2/(N_o - N_v)]^{1/2}$ where N_o and N_v are, respectively, the number of observations and variables.

eters and the remainder of the crystallographic data are provided as supporting information.

Results and Discussion

Sodium iron(III) ethylenediamine tetraacetate (NaFeEDTA) is a readily prepared and commercially available reagent that is very attractive for the purpose of preparation of a crystalline ferrite precursor. For example, it can be expected that reaction with a divalent metal would result in a salt with a 1:2 M^{2+}:Fe ratio (eq 1).

$$MX_2 + 2NaFeEDTA \rightarrow M(FeEDTA)_2 + 2NaX \quad (1)$$

However, the anion is so large that its selectivity for a divalent cation over a monovalent one is low. Therefore, in practice a compound crystallizes which contain sodium and a reduced amount of the divalent metal (eq 2).

$$MX_2 + 2NaFeEDTA \rightarrow Na_{2x}M_{1-x}(FeEDTA)_2 \quad (2)$$

For example, the reaction of nickel(II) nitrate with 2 mol equiv of NaFeEDTA produces a crystalline compound with very little nickel; ICP spectroscopic analysis indicated a composition of $Na_{1.82}Ni_{0.08}(FeEDTA)_2$. With 5 times the stoichiometric amount of Ni^{2+} the substitution of nickel for sodium improves, but only to a nickel-to-iron ratio of 1:2.55 [i.e., $Na_{0.44}Ni_{0.78}(FeEDTA)_2$].

One solution to the problem of sodium contamination is to remove all sodium from the system in the first place. This could be accomplished by replacing sodium ions with protons which may subsequently be removed readily during pyrolysis and, therefore, have no potential for contaminating the final ceramic material. Protonated iron(III) ethylenediamine tetraacetate (HFeEDTA) may be prepared by literature routes,[13] but solutions of it may also be conveniently prepared by treatment of NaFeEDTA with a protonated ion exchanger. Thus, passing a 0.10 M solution of NaFeEDTA through an excess of protonated Amberlite resin reduces the sodium concentration to 0.95 ppm.

Addition of nickel(II) chloride to a solution of HFeEDTA (in a 1:2 molar ratio) followed by slow evaporation of the water leads to growth of large (up to 1 cm) transparent green crystals of hydrated $[Ni(H_2O)_6][FeCl(HEDTA)]_2$. When crushed, the crystals yield a yellow powder with a slight greenish tinge. If left exposed to ambient air, this powder gradually darkens to a greenish brown color. This process is tremendously accelerated in a flow of dry nitrogen and may be attributed to dehydration. It may be noted that dilute aqueous solutions of this compound are yellow in color and exhibit two UV−visible absorption maxima at 204 nm (ϵ = 13 800) and 258 nm (ϵ = 15 300). In more concentrated solutions a third absorption is observed at 406 nm (ϵ = 104). The two lower wavelength absorptions may be attributed to MLCT transitions in the anion since similar bands are observed for HFeEDTA at 206 and 256 nm.

The as-prepared crystals of **1** were found to contain four waters of hydration in addition to the six surrounding nickel (i.e., ten in total). This was confirmed both by elemental analysis and dehydration measurements on a thermogravimetric analyzer (see below). When exposed to ambient air, the crystals lost water very slowly and gradually turned brown along the edges. However, the X-ray powder diffraction pattern of the crystals remained unaffected by these changes, and the crystal which was eventually selected for single-crystal X-ray diffraction was found to contain only eight waters (see below). There was excellent agreement between the analytical results for all of the non-oxygen elements and those calculated for the formula $[Ni(H_2O)_6][FeCl(EDTA)H]_2\cdot 4H_2O$. Of particular importance to the application of this compound for the preparation of nickel ferrite, ICP spectroscopy indicated that a ratio of nickel to iron of 1:2.01. This ratio was also very consistant between separate preparations of **1**.

The presence of water is evident in the infrared spectrum of **1** in which absorptions at 1675 and 3498 cm^{-1} are observed for the bending and stretching modes of water, respectively. The latter peak is somewhat masked by the broad adsorption due to the O−H stretch of the protonated carboxylate, which is centered at 3294 cm^{-1}. Additionally, bands due to the C−O stretch of the protonated, uncoordinated carboxylate is observed at 1728 cm^{-1}. The corresponding band is observed at 1758 cm^{-1} in HFeEDTA.[12] As well, Morris and Busch reported an absorption at 1745 cm^{-1} for this moiety in sodium nitro(hydrogenethylenediaminetetraacetato)-cobalt(III) monohydrate.[14] The corresponding absorption for the deprotonated, coordinated carboxylates is found at 1628 cm^{-1}. This band is most easily resolved and identified in vacuum-dried crystals.

X-ray Crystal Structure of $[Ni(H_2O)_6][FeCl(EDTA)H]_2\cdot 2H_2O$. Intramolecular bond distances and bond angles are given in Tables 2 and 3, respectively. The crystal structure of **1** consists of layers of [Ni-

(13) Kennard, C. H. L. *Inorg. Chim. Acta* **1967**, *1*, 347.
(14) Morris, M. L.; Busch, D. H. *J. Am. Chem. Soc.* **1956**, *78*, 5178.

Table 2. Bond Distances (Å) for $[Ni(H_2O)_6][FeCl(C_{10}H_{13}O_8N_2)]_2\cdot 2H_2O$[a]

Ni−O(1)	2.028(2)	O(8)−C(8)	1.286(3)
Ni−O(2)	2.061(2)	O(9)−C(8)	1.232(3)
Ni−O(3)	2.073(2)	O(10)−C(10)	1.226(3)
Fe−Cl	2.2517(7)	O(11)−C(10)	1.282(3)
Fe−O(6)	1.964(2)	O(12)−H(20)	0.89(5)
Fe−O(8)	2.002(2)	O(12)−H(21)	0.73(4)
Fe−O(11)	2.001(2)	O(13)−H(22)	0.85(4)
Fe−N(1)	2.205(2)	O(13)−H(23)	0.75(4)
Fe−N(2)	2.210(2)	N(1)−C(1)	1.496(3)
O(1)−H(14)	0.89(4)	N(1)−C(3)	1.481(3)
O(1)−H(15)	0.83(4)	N(1)−C(5)	1.493(3)
O(2)−H(16)	0.83(4)	N(2)−C(2)	1.487(3)
O(2)−H(17)	0.81(3)	N(2)−C(7)	1.474(3)
O(3)−H(18)	0.76(3)	N(2)−C(9)	1.479(3)
O(3)−H(19)	0.87(4)	C(1)−C(2)	1.511(4)
O(4)−C(4)	1.311(4)	C(3)−C(4)	1.512(3)
O(4)−H(13)	0.74(5)	C(5)−C(6)	1.516(4)
O(5)−C(4)	1.200(3)	C(7)−C(8)	1.517(3)
O(6)−C(6)	1.282(3)	C(9)−C(10)	1.512(3)
O(7)−C(6)	1.228(3)		

[a] Numbers in parentheses are estimated standard deviations in the least significant digits.

Table 3. Bond Angles (deg) for $[Ni(H_2O)_6][FeCl(C_{10}H_{13}O_8N_2)]_2\cdot 2H_2O$[a]

O(1)−Ni−O(2)	88.87(9)	H(16)−O(2)−H(17)	101.(3)
O(1)−Ni−O(3)	91.21(9)	Ni−O(3)−H(18)	116.(3)
O(2)−Ni−O(3)	91.82(8)	Ni−O(3)−H(19)	115.(2)
Cl−Fe−O(6)	99.28(6)	H(18)−O(3)−H(19)	104.(3)
Cl−Fe−O(8)	100.25(5)	C(4)−O(4)−H(13)	107.(4)
Cl−Fe−O(11)	94.67(5)	Fe−O(6)−C(6)	120.1(2)
Cl−Fe−N(1)	101.38(6)	Fe−O(8)−C(8)	118.8(1)
Cl−Fe−N(2)	173.47(5)	Fe−O(11)−C(10)	119.3(1)
O(6)−Fe−O(8)	89.62(7)	H(20)−O(12)−H(21)	99.(4)
O(6)−Fe−O(11)	165.06(7)	H(22)−O(13)−H(23)	101.(4)
O(6)−Fe−N(1)	80.10(7)	Fe−N(1)−C(1)	106.7(1)
O(6)−Fe−N(2)	86.85(7)	Fe−N(1)−C(3)	109.8(1)
O(8)−Fe−O(11)	93.15(7)	Fe−N(1)−C(5)	104.7(1)
O(8)−Fe−N(1)	157.28(7)	C(1)−N(1)−C(3)	111.7(2)
O(8)−Fe−N(2)	77.40(7)	C(1)−N(1)−C(5)	111.7(2)
O(11)−Fe−N(1)	91.98(7)	C(3)−N(1)−C(5)	111.8(2)
O(11)−Fe−N(2)	79.45(7)	Fe−N(2)−C(2)	105.9(1)
N(1)−Fe−N(2)	81.81(7)	Fe−N(2)−C(7)	104.7(1)
Ni−O(1)−H(14)	114.(2)	Fe−N(2)−C(9)	108.4(1)
Ni−O(1)−H(15)	122.(3)	C(2)−N(2)−C(7)	114.3(2)
H(14)−O(1)−H(15)	114.(3)	C(2)−N(2)−C(9)	111.9(2)
Ni−O(2)−H(16)	113.(3)	C(7)−N(2)−C(9)	111.0(2)
Ni−O(2)−H(17)	116.(2)	N(1)−C(1)−C(2)	111.9(2)
N(2)−C(2)−C(1)	110.0(2)	N(2)−C(7)−C(8)	109.6(2)
N(1)−C(3)−C(4)	116.4(2)	O(8)−C(8)−O(9)	123.1(2)
O(4)−C(4)−O(5)	125.0(3)	O(8)−C(8)−C(7)	116.1(2)
O(4)−C(4)−C(3)	110.0(2)	O(9)−C(8)−C(7)	120.7(2)
O(5)−C(4)−C(3)	125.0(2)	N(2)−C(9)−C(10)	113.0(2)
N(1)−C(5)−C(6)	111.9(2)	O(10)−C(10)−O(11)	124.1(2)
O(6)−C(6)−O(7)	124.2(2)	O(10)−C(10)−C(9)	118.6(2)
O(6)−C(6)−C(5)	116.4(2)	O(11)−C(10)−C(9)	117.3(2)
O(7)−C(6)−C(5)	119.4(2)		

[a] Numbers in parentheses are estimated standard deviations in the least significant digits.

$(H_2O)_6]^{2+}$ cations lying in the *bc* plane and bounded on either side by double layers of $[FeCl(C_{10}H_{13}O_8N_2)]^-$ anions (Figure 1). The cation has crystallographically imposed $\bar{1}$ symmetry and is associated with neighboring cations via hydrogen bonding to one of the solvent water molecules. Both this water molecule and two of those coordinated to nickel hydrogen bond to the EDTA ligand of the anion. The second solvent water molecule, which lies between adjacent anion layers, is hydrogen bonded to the proton on O(4) of the uncoordinated arm of this ligand (Table 4). A perspective view of the anion is given in Figure 2, from which it is evident that the coordination about iron is significantly distorted from octahedral. The primary distortion is a bending of the

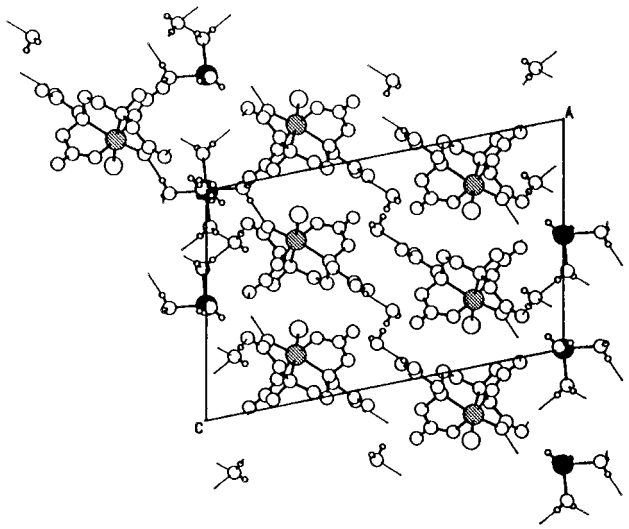

Figure 1. Crystal packing diagram of **1** viewed down the *b* axis. Black circles are nickel atoms, while gray ones are iron.

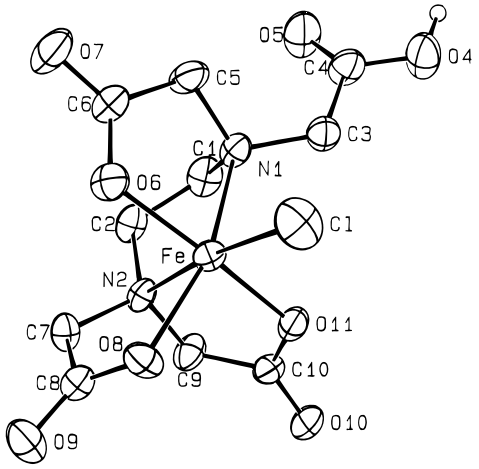

Figure 2. Perspective view of the $[FeCl(C_{10}H_{13}O_8N_2)]^-$ anion. Thermal ellipsoids are drawn at the 50% probability level, and hydrogen atoms attached to carbon are omitted for clarity.

Table 4. Hydrogen Bonds in $[Ni(H_2O)_6][FeCl(C_{10}H_{13}O_8N_2)]_2\cdot 2H_2O$

O_A, H_B	$O_A\cdots H_B$ (Å)	$H_A-O_A\cdots H_B$ (deg)
O(12), H(13)[a]	1.91(5)	165(5)
O(8), H(16)[b]	1.92(4)	169(3)
O(9), H(19)	1.90(4)	175(3)
O(9), H(22)[c]	1.93(4)	153(4)
O(10), H(17)[d]	1.93(3)	161(3)
O(13), H(14)[d]	1.84(4)	167(4)
O(13), H(15)[e]	1.95(4)	169(4)

[a] At $1 + x$, $-1/2 + y$, $3/2 + z$. [b] At $-x$, $-y$, $-z$. [c] At $-x$, $-1/2 + y$, $-1/2 - z$. [d] At x, $1/2 - y$, $1/2 + z$. [e] At x, y, $1 + z$.

four substituents cis to the chloride away from the latter (Table 3). A similar distortion appears to be present in the closely related $[RuCl(C_{10}H_{13}O_8N_2)]^-$ anion, but few structural details on the latter are available for comparison.[15] The Fe−Cl distance is somewhat shorter than the average value of 2.308 Å found previously for six-coordinate Fe(III) complexes.[16]

The coordination of the EDTA ligand to iron in **1** is quite similar to that reported for $HFeEDTA\cdot H_2O$.[13] In

(15) Taqui Khan, M. M.; Chatterjee, D.; Merchant, R. R.; Paul, P.; Abdi, S. H. R.; Srinivas, D.; Siddiqui, M. R. H.; Moiz, M. A.; Bhadbhade, M. M.; Venkatasubramanian, K. *Inorg. Chem.* **1992**, *31*, 2711.

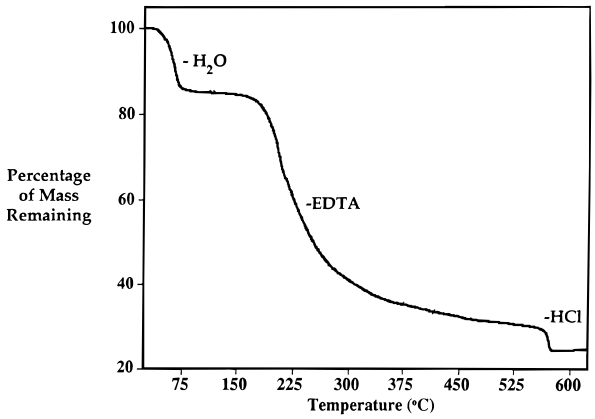

Figure 3. Thermogravimetric analysis of **1** in dry air at 1 °C/min.

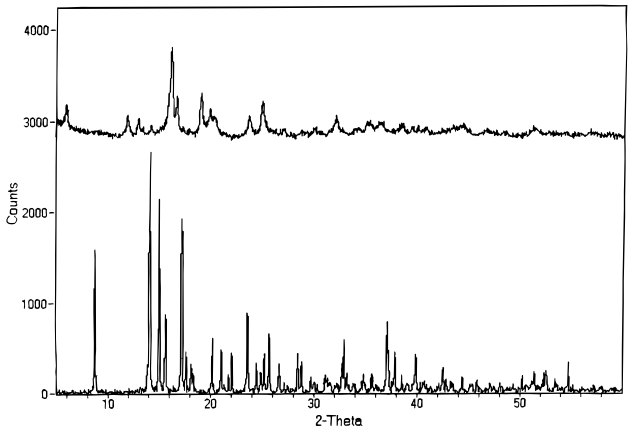

Figure 4. X-ray diffraction patterns of (a) as-prepared $[Ni(H_2O)_6][FeCl(EDTA)H]_2 \cdot 4H_2O$ and (b) the same material dried at 140 °C for 12 h.

the latter, the sixth coordination site of the iron is occupied by a water molecule rather than chloride. The average iron−oxygen (1.989 vs 1.98 Å) and iron−nitrogen (2.209 vs 2.22 Å) bond distances are comparable. However, it should be noted that both complexes exhibit significant variation in the metal−ligand bond lengths.

While both **1** and $HFeEDTA \cdot H_2O$ have structures that consist of layers of iron ethylenediamine complexes, they differ in how the complexes are arranged. In $HFeEDTA \cdot H_2O$, the proton on the free arm of the EDTA ligand hydrogen bonds to an adjacent anion within the same layer,[13] while in **1** these protons tie adjacent layers of anions together by hydrogen bonding to the interlayer water molecules.

Thermal Decomposition of 1. The thermogravimetric analysis of uncrushed crystals of **1** is shown in Figure 3. Use of these crystals rather than ground powder allows the degree of hydration to be determined since the powdered material loses 6 mol equiv of water under the dry air flow at 25 °C, making it difficult to obtain the proper initial weight. The first transition in the TGA of the crystals is loss of water molecules between the temperatures 80 and 140 °C.

The dehydration of a bulk sample of **1** at 140 °C yields a solid that is still crystalline as evidenced by X-ray powder diffraction. Of course, major changes in the structure have occurred, and the patterns of the initial and dehydrated compounds are markedly different (Figure 4). The next weight loss is exothermic and corresponds to decomposition and oxidation of the EDTA ligand. Its onset is at 194 °C and is similar to the decomposition point of free EDTA which begins to decarboxylate at 150 °C.[17] The infrared spectrum of a bulk sample of **1** pyrolyzed just above this temperature (200 °C) indicates that this decomposition is accompanied by the disappearance of the C−O stretch for the protonated carboxylate moiety. Therefore, it may be assumed that, at least in part, the initial decomposition of the ligand is due to decarboxylation of the protonated carboxylate. In this investigation, support for this conclusion was provided by thermal gravimetric analysis which demonstrated that HFeEDTA decarboxylates at 184 °C. However, it should be noted that other degradation reactions of EDTA also occur at very similar temperatures, e.g., the dianhydride of EDTA melts with decomposition at 190 °C.[18] The only volatiles identifiable by simultaneous analysis of the off-gases by mass spectroscopy are carbon dioxide, nitrogen dioxide, and water. In an attempt to identify any nonvolatile neutral organics that are produced at this temperature, a bulk sample was pyrolyzed in a sealed container, and the resulting solid was extracted with diethyl ether. GC/MS analysis of this mixture revealed a rather complex mixture of compounds, none of which could be identified using the NIST database. However, the majority of the substances were carboxylic acid derivatives as indicated by the predominance of a peak for CO_2^+ ($m/e = 44$) in their mass spectra. These are possibly a variety of both cyclic and acyclic anhydrides produces by extrusion of iron oxide (eq 3).

$$2R{-}CO_2Fe \rightarrow R{-}C(O)OC(O){-}R + Fe{-}O{-}Fe \quad (3)$$

The removal of the EDTA ligand occurs gradually over a broad temperature range and is fairly complete by 300 °C. At this point, XRF analysis of a sample pyrolyzed in bulk indicates that the precise ratio of nickel to iron has been maintained. As well, all of the original chloride is still present. This is surprising, since iron oxychloride, FeOCl, dissociates to iron oxide and volatile iron(III) chloride at 300 °C.[19] Also infrared spectroscopy indicates that hydroxide anions are still present in the solid with absorptions at 3310 and 1586 cm^{-1}. However, nickel hydroxide dehydrates at 230 °C,[20] while iron oxide hydroxide dehydrates above 250 °C.[21] It appears, therefore, that the solid must consist of one or more phases that are unlike the separate oxychlorides or hydroxides. However, what these might be cannot be ascertained since X-ray powder diffraction indicates that the solid is amorphous.

Beyond 300 °C little change in weight is observed until 576 °C, when an abrupt exothermic change occurs which corresponds to the loss of 2 equiv of HCl. TGA/MS and a litmus paper test confirms the identify of this

(16) Orpen, A. G.; Brammer, L.; Allen, F. H.; Kennard, O.; Watson, D. G.; Taylor, R. *J. Chem. Soc., Dalton Trans.* **1989**, S1.

(17) *The Merck Index*, 11th ed.; Budaveri, S., O'Neil, M. J., Smith, A., Eds.; Merck & Co.: Rahway, NJ, 1989; p 550.

(18) Geigy, J. R. French Patent 1,548,888, 1968.

(19) Schäfer, H. *Z. Anorg. Chem.* **1949**, *260*, 279.

(20) Glemser, O. In *Handbook of Preparative Inorganic Chemistry*; Brauer, G., Ed.; Academic Press: New York, 1965; Vol. 2, p 1549.

(21) Lux, H. In *Handbook of Preparative Inorganic Chemistry*; Brauer, G., Ed.; Academic Press: New York, 1965; Vol. 2, p 1501.

gas. Correspondingly, XRF analysis of a bulk sample of **1** pyrolyzed at 600 °C demonstrates that all chloride has been lost from the solid. Again, the ratio of nickel-to-iron has remained unchanged. At this point, X-ray powder diffraction indicates that the solid is crystalline and consist of two phases: a minor Fe_2O_3 (hematite) phase and nickel ferrite. Since the overall ratio of the metals is still 1Ni:2Fe, either the latter phase is nonstoichiometric (i.e., nickel rich) or, more likely, amorphous phases are still present. Further heating to 900 °C is required in order to convert the solid to phase-pure nickel ferrite. Obviously, the kinetics of this step are limited by solid-state diffusion, but nevertheless the XRF spectroscopy indicates that the final product is highly stoichiometric $NiFe_2O_4$ with a nickel-to-iron ratio of 1:2.01.

The formation of the two intermediate phases is not surprising considering the tremendous rearrangement of the inorganic lattice which must occur in the formation of nickel ferrite from **1**. Soft ferrites belong to a large class of compounds, AB_2X_4, whose structures are related to spinel, $MgAl_2O_4$. The unit cell of spinels contains a cubic close-packed array of 32 oxygen atoms. In the normal spinel structure, the eight "A" metal atoms occupy tetrahedral sites, while the "B" metal atoms occupy octahedral salts. However, nickel ferrite has an inverse spinel structure where the nickel atoms occupy the B sites, and the iron atoms are therefore distributed over both the octahedral and tetrahedral sites. As a result, $NiFe_2O_4$ consists of planes of metals that alternate: Fe−(Ni,Fe)−Fe−(Ni,Fe). Thus, the array of metals in the precursor (alternating planes of Ni−Fe−Fe−Ni−Fe−Fe) must undergo complete rearrangement in order to form crystalline $NiFe_2O_4$. However, the retention of chloride during pyrolysis may also contribute to phase segregation, but the significance of the chloride's role remains undetermined.

Conclusion

The reactions of nickel(II) salts with NaFeEDTA and HFeEDTA have been investigated, and it has been found that a water-recrystallizable stoichiometric precursor for nickel ferrite may be synthesized by the reaction of nickel(II) chloride with NaFeEDTA. The $[Ni(H_2O)_6][FeCl(EDTA)H]_2 \cdot 2H_2O$ thus obtained has an interesting layered structure in which the nickel-to-iron ratio is fixed at a 1:2 ratio. The dehydration of this compound and removal of the EDTA by pyrolysis at 300 °C result in an amorphous phase in which the chloride ions and hydroxide residues are retained. These are lost upon heating to 600 °C, leaving a residue that consists of $NiFe_2O_4$ and Fe_2O_3. Crystalline, stoichiometric nickel ferrite is obtained only upon heating to 900 °C.

Acknowledgment. We thank the Louisiana Board of Regents for support through the Louisiana Educational Quality Support Fund Contract LEQSF(1993-96)-RD-A-26. We also express gratitude to Tulane's Coordinated Instrument Facility for the provision of analytical services and technical assistance.

Supporting Information Available: Final refined parameters, tables of anisotropic thermal parameters and calculated hydrogen positional parameters (6 pages); tables of calculated and observed structure factors (14 pages). Ordering information is given on any current masthead page.

CM9503590